Characterisation and laboratory investigation of a new ultraviolet multi-wavelength measuring system for high-temperature applications

Characterisation and laboratory investigation of a new ultraviolet multi-wavelength measuring system for high-temperature applications

M. Battuello* **and F. Girard**
Istituto Nazionale di Ricerca Metrologica (INRIM), Strada delle Cacce 91, Torino, Italy

*Corresponding author. Tel: +39 011319738
E-mail address: *m.battuello@inrim.it*

Abstract. In the framework of the HiTeMS project of the European Metrology Research Pogramme (EMRP) a new multi-wavelength device for measurement of high temperatures in industrial applications was developed at INRIM. The apparatus takes advantage of the ultra-violet operation with working wavelengths from 350 nm up, which reduces the possible errors connected with the multi-wavelength approach. The instrument has been characterised in terms of optical and electronic behaviour and some laboratory trials were carried out to verify the reliability of the multi-wavelength approach. The true temperature of a blackbody source at 1300 °C with optical windows of unknown spectral transmittance interposed has been defined. By applying an approach that allows a result to be accepted when a threshold limit is reached, it was found that, when an acceptable result can be obtained, errors are comprised within less than 1 % of the temperature of the source. Three others single-band thermometers, at 508 nm, 650 nm and an IR broadband 0.8 µm-1.1µm, were also used to the purpose of a comparison. It has been found that, when the multi-wavelength approach is applicable, it provides generally better or in few cases, at worst similar results of corrected single-wavelength thermometers.

Keywords: radiation thermometry, multi-wavelength, emissivity

1. Introduction

Radiation thermometry is a non-contact method, hence it is robust and, in principle, suitable for high-temperature applications in a broad spectrum of industries. However, it is well known that when radiation thermometers are used in practical applications outside laboratories the uncertainty rapidly increases because of the measurement environment. The unknown emissivity of the surface under investigation is the most common source of uncertainty, but also unknown absorption along the optical path or the transmission of possible protective windows used in the measurement setups may play an important role. Many attempts have been made over the years to overcome these problems, but no generally applicable method has been devised. If we refer to the emissivity issue, but the reasoning is the same for the other influencing parameters, increasing the number of measuring wavelengths, and provided that some assumptions on the emissivity behaviour are done, it is possible, in principle, to derive the real temperature of a surface from the spectral radiances measurements.

The approach can be implemented by means of different experimental methods. Before the advent of the array detectors, it was common practice to split /select the incoming radiation by means of optical filters with the consequent limitation of operating at few and fixed working wavelength bands. Nowadays the use of array detectors allows to realize a device to be used directly as a multi-wavelength thermometer with a high degree of flexibility both in terms of number and position of the working wavelengths bands. However, in practice these advantages are not sufficient to make the multi-wavelength approach a reliable one for operations in the Visible-Near Infrared (VIS-NIR), i.e., in spectral ranges normally used for measurement of temperatures around 1000 °C or less. The attempts made to develop practical thermometers were not satisfactory because of the unreliability of the results. A dependence of the results on the specific material under measurement was found and there was no practical means to know the extent of the possible errors. However, an analysis of the measuring principle of the multi-wavelength thermometry, suggested the opportunity to investigate the possible advantages in extending the operating wavelengths down to the ultra-

violet. The multi-wavelength approach essentially is an extrapolation process towards $\lambda \rightarrow 0$ of measurement data obtained in a defined spectral range. Such considerations may suggest that by reducing the extrapolation range it should be possible to reduce the errors. Based on this assumption simulations were performed and consistent improvements were found [1]. On such basis, INRIM developed for the High Temperature Metrology for Industrial Applications (HiTeMS) project of the European Metrology Research Programme (EMRP) a flexible multi-wavelength measuring system for high temperature applications. The instrument was constructed to be operated in a spectral range comprised between 350 nm and 950 nm.
Functionality tests and measurements have been performed in different setup conditions in order to characterize the device. The tests referred both to the electronic and optics-related characteristics of the device. The characterization evidenced some limitations, particularly referred to the electronics. The linearity of the gain ratios and exposure times of the CCD detector strongly depends by the wavelength. Such a behavior makes difficult to manage signals with large dynamic range as those available when wide spectral regions are analyzed and consequently an alternative operative approach was devised to overcome these electronic drawbacks. However, an important outcome of the characterization was the extremely high sensitivity of the device that open to lower temperatures operation with respect to the originally expected limits. It has been found that the MWT can be operated at temperatures as low as 1300 °C with the originally set spectral limits, i.e., 350 nm - 950 nm, and even down to 900 °C if the minimum operating wavelength is increased to 500 nm.
The paper will briefly discuss the measurement principle, will describe the apparatus, its characterization and some laboratory investigations simulating industrial trials aimed to compare the results with those obtainable with common single-wavelength radiation thermometers at different wavelengths.

2. Discussion of the measurement principle

An analysis of the measurement principles can be found in [1]. In radiation thermometry when N measuring wavelengths are used a general representation with a system of N equations with N+1 unknowns can be derived and by conveniently using the Wien's approximation of the Planck's equation:

$$L_{\lambda_i,T}(\varepsilon_{\lambda_i}) = \varepsilon_{\lambda_i}\, c_1\, \lambda_i^{-5} \exp\left(-\frac{c_2}{\lambda_i T}\right) \tag{1}$$

where $i = 1, \ldots N$ is the number of wavelengths used, λ is the wavelength, c_1=1.1911x10^{-16} W·m^{-2}·sr^{-1} and c_2=1.4388x10^{-2} m·K are the first and second radiation constant, respectively, T is the temperature in kelvin and $\varepsilon_{\lambda i}$ are the spectral emissivities. By assuming the emissivity to be a function of the wavelength with no more than N-1 coefficients, the system of equations will contain no more than N unknowns and consequently can be analytically solved. As suggested by Coates [2] the following polynomial expression with a degree $M \leq N-2$ can be used to describe the emissivity behaviour:

$$\ln \varepsilon_\lambda = \sum_{j=0}^{j=M} a_j \lambda^j \tag{2}$$

The spectral radiances can be written down in a straight way and all the following calculation process can be consequently greatly simplified. By combining eq. (1) and eq. (2) the following equation can be obtained:

$$Y_i = \frac{c_2}{T} - \lambda_i \sum_{j=0}^{j=M} a_j \lambda_i^j \tag{3}$$

where:

$$Y_i = \lambda_i \left[-\ln L_{\lambda,T}(\varepsilon_\lambda) + \ln c_1 - 5 \ln \lambda_i \right] \tag{4}$$

are the measured radiance terms. Consequently, the temperature and the emissivity can be simultaneously derived by solving the system of equations described above.

In practice, searching for the value of temperature T in the equation (3) corresponds to search for the value of the function Y_i when the wavelength λ tends to zero:

$$\lim_{\lambda \to 0}\left(\frac{c_2}{T} - \lambda_i \sum_{j=0}^{j=M} a_j \lambda_i^j\right) \tag{5}$$

and the equation (3) assumes the form:

$$T = \frac{c_2}{Y_i} \tag{6}$$

The calculation procedure appears to be as an extrapolation process towards $\lim \lambda \to 0$. The system of equations to be solved can be expressed and written in a matrix form, as shown in the section 5.2

3. Description of the multi-wavelength measuring system

The multi-wavelength measuring system has been based on a 1024 x 256 elements CCD silicon detector (HJY model Syncerity™) and an automated spectrometer (HJY model MicroHRauto) coupled together to form a complete spectrometric system. Both devices are produced and commercially available from Horiba Scientific. In addition to the two instruments, a dedicated input optics has been designed for the specific application to be positioned in front of the spectrometer's input slit. A picture of the system is shown in Figure 1.

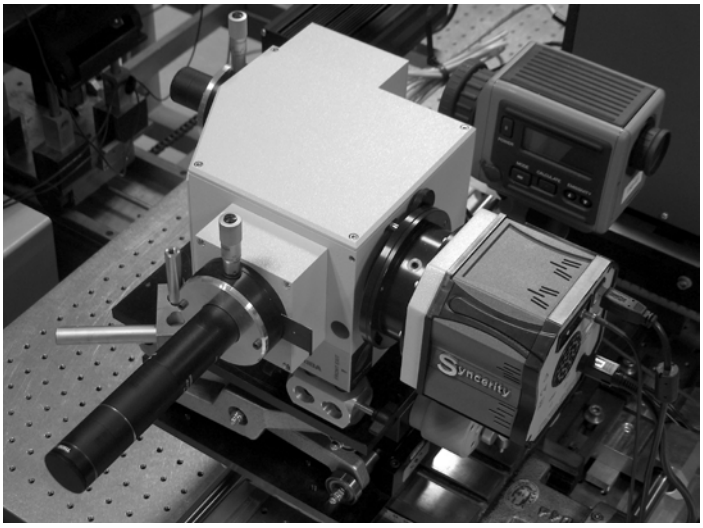

Figure 1. Picture of the multi-wavelength system

3.1 The Syncerity CCD detector

The core of the detection system is a Scientific Grade 1 - CCD array (model E2V CCD30-11-1-275), thermoelectrically cooled down to - 60 °C to minimize the dark current contribution, mounted inside a detector head provided with a metal sealed technology that guarantee a life-time maintenance-free vacuum. The array detector has 26 μm x 26 μm pixel size with 100 % fill factor and it is sensitive in the wavelength range from 250 nm (with a QE = 27 %) up to 1050 nm. The data acquisition electronic of the CCD detector allows the settings of three different gain levels: High Sensitivity, Best Dynamic and High Light each with an exposure time control ranging from 1 ms up to 262.14 s and performs the AD conversion with a nominal resolution of 16 bits (Note: the true final resolution of the system depends on the real full well capacity of the node shift register in conjunction with the gain level setting). Even if the CCD array can work in "image mode" giving a bi-dimensional information of the image at the exit port of the spectrometer, during the measurements it has been used only in "spectral mode" by means of its electronic function of vertical binning of a certain number of pixel's rows.

3.2 The MicroHRauto spectrometer

The instrument has based on a Czerny-Turner layout with focal length of 140 mm and toroidal collimating mirror. The entrance aperture is *f* / 3.9 and the input slit is a micrometric one with size adjustable from 10

μm up to 2 mm. Two different gratings can be mount on an interchangeable turret. The scanning range is from 0 nm to 1500 nm with a drive speed of 500 nm / s.
For the present purpose, after an initial tuning of the entire system, the spectrometer has been used and kept fixed in the following configuration: input slit size of 0.1 mm, grating with 300 grooves/mm and central wavelength positioned at 650 nm. With such settings the working bandwidth covers exactly the range of wavelengths from 350 nm up to 950 nm.

3.3 The input optics

Previous experiences in designing radiation thermometers, suggested that for laboratory operation in front of radiation sources at relatively high temperatures, a working distance of about 700 mm can be adequate. Even if, in principle, the aperture ratio of the input optic of a measuring instrument should be as large as possible, experimental evidences suggested that considered the high sensitivity of the CCD detector, a less demanding need is to keep the aperture ratio of the optical input stage equal to that of the MicroHRauto spectrometer (f / 3.9). The scope of an input optics is to collect the thermal radiation from the temperature source. The aperture, together with the size of the spectrometer's input slit, defines both the solid angle and a well defined area under which the radiance source is observed. Thanks to the high sensitivity of the CCD detector and to optimize both the size of source contribution and the optical transmission especially at the short wavelengths, a simple pinhole camera design with a narrow f number ($\cong f$ / 100) has been adopted for the measurement exercise here described. By using such a technique, the dimensions of the field of view of the MWT can be geometrically determined by knowing both sizes and relative positioning distance between the pinhole and the spectrometer's input slit. Neglecting the contribution from diffraction at the apertures, a square shaped field-of-view of 8.4 mm x 8.4 mm has been determined at the chosen working distance of 680 mm. Before each measurement run the alignment of the multi-wavelength system has been checked by setting the spectrometer's grating at order zero in wavelength, i.e., the CCD in "image mode, and by observing that the shape of the radiance source is symmetrically located with respect to both horizontals and verticals centrals rows of pixels of the CCD detector.

4. Characterization of the MWT

The device has been characterised with respect to its optical and electronic performances. Preliminary investigations on the latter evidenced some unexpected behaviour difficult to manage. The next section on linearity will discuss the issue.

4.1 Linearity

The linearity of the output signal depends on the detection of the radiant fluxes and on the successive electronic processing of the photocurrents. It has been found that the system is affected by a strong, and not clearly explained, non-linearity in terms of both wavelength and number of counts, associated to the exposure times and to the gain ratios. Such behavior makes the characterization a complicated task and hence it was decided for a different operative approach to overcome the difficulty. In practice, to calibrate the device means to measure the spectral response curve of the system and then to derive the spectrum of the source under investigation through the former by using different exposure times and gain ratios. A possible alternative consists in deriving different spectral responses associated to a discrete number of exposure times to be used successively during the measurements. In practice, a blackbody source at different known temperatures is used with an exposure time such that the maximum number of counts of the measured output curve is near to the saturation, namely at about 60000 counts. The response curve of the system is then simply derived by dividing the output curve by the Planck's curve at that temperature. Such a procedure simplify the measurements because allows to operate directly with the same exposure time used for the calibration and consequently avoids any needs for a calibration in terms of exposure time ratios.
However, because of the high dynamic range of the measured signals, each spectrum may contain in practice signals from few tens of counts to near the saturation and consequently the possible non-linearity related to the number of counts with the same exposure time need to be verified. To this purpose, the procedure described in the next section 4.1.1 has been followed.

4.1.1 Nonlinearity measurement system

A dual-aperture device (DAD), shown in Figure 2, was used for the measurements [3]. With such a method, a single radiation source is needed and the radiation beam from it is divided by a rotating shutter. A LAND Calibration Source model R1500T provided with six SiC heaters were used as a radiation source. The

furnace was modified and improved at INRIM where a SiC cavity with 45 mm internal diameter and 95 mm length was constructed. For the present exercise a ϕ 15 mm diaphragm was placed at the aperture of the furnace. In these conditions the calculated effective emissivity of the cavity is greater than 0.998.

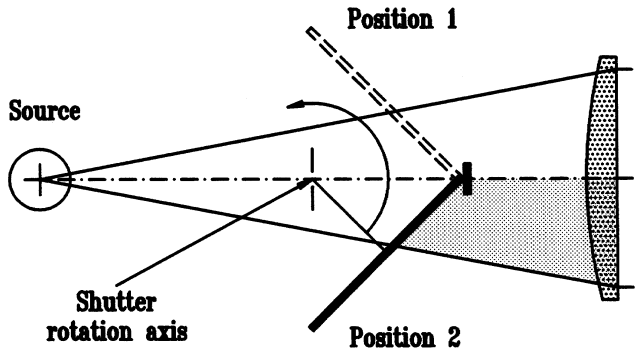

Figure 2. Operational scheme of the DAD device for nonlinearity measurements

In general, at any photocurrent value i_{A+B} generated by the simultaneous detection of the two flux components, the nonlinearity function $NL(i_{A+B})$ is defined as

$$NL(i_{A+B}) = [i_{A+B} - (i_A + i_B)] / i_{A+B}$$

where i_A and i_B are the photocurrents generated by the corresponding flux components. In the present exercise we are interested in measuring the *NL* on the output counts for different exposure times. To this purpose, the furnace was set to 1300 °C and three different exposure time, namely 700 ms, 2.25 s and 5 s, were selected. The exposure times were selected in such a way to just get a wide spectrum of counts at the different wavelengths and consequently is of no significance that with 5 s there is a saturation of the number of counts for wavelengths longer than 650 nm.The corresponding output curves shown in Figure 3 were detected.

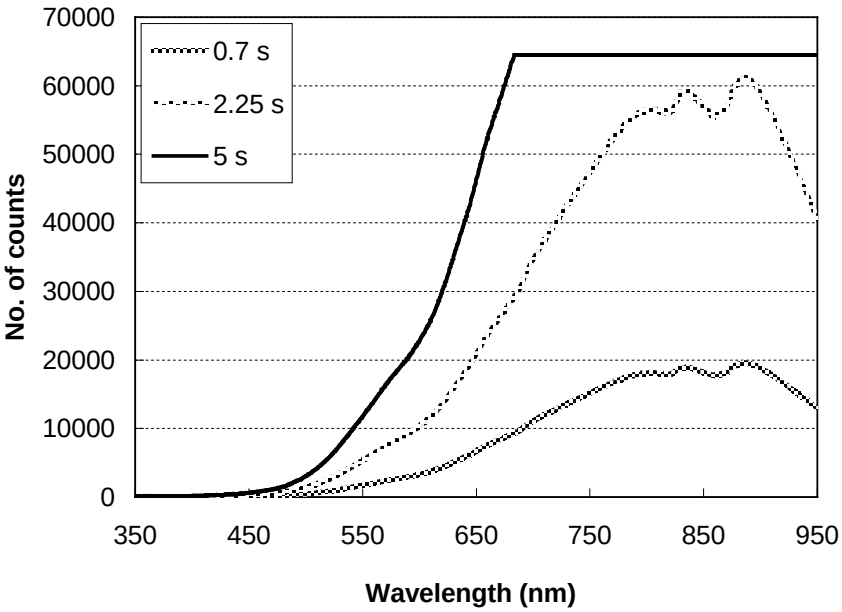

Figure 3. Output curves obtained with three different exposure times

Figure 4 shows the nonlinearity in terms of counts and independently of the wavelength, i.e., for a specific number of counts are reported *NL* values at different wavelengths. For example, at 20000 counts there are *NL* values at 590 nm, 650 nm and 890 nm, as can be easily inferred from Figure 3. A check on the possible influence of the DAD on the measured *NL* was made by tilting it ±2.5 ° with respect to the orthogonal position. Some slight variation within ±0.4 % was found. The data reported in Figure 4 immediately suggest

that there is no evident *NL* related to the number of counts. To better analyse the data, all the *NL* values have been averaged and a linear fitting, shown with the line in the figure, have been calculated. The line is substantially parallel to *NL*=0 but with a slight shift of about -0.5 % which is probably due to a measurement uncertainty.

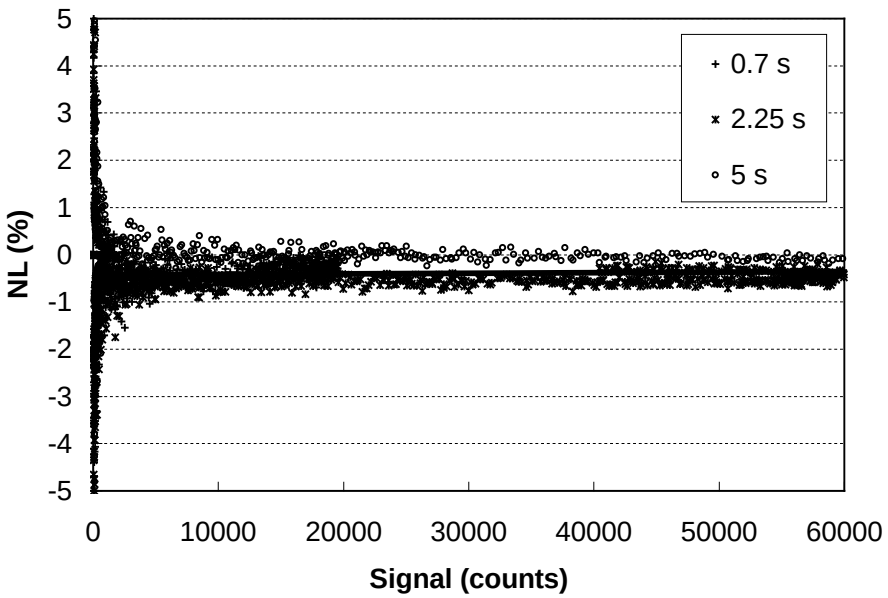

Figure 4. Nonlinearity in terms of number of counts and independently of the wavelength

Figure 5 shows the nonlinearity in terms of wavelength and irrespective of the number of counts. Figures 4 and 5 evidence that no appreciable counts- and wavelength-related nonlinearities are present, respectively. In the low signal range, i.e., at short wavelengths up to about 450-500 nm, variations of *NL* related to the noise signal are present.

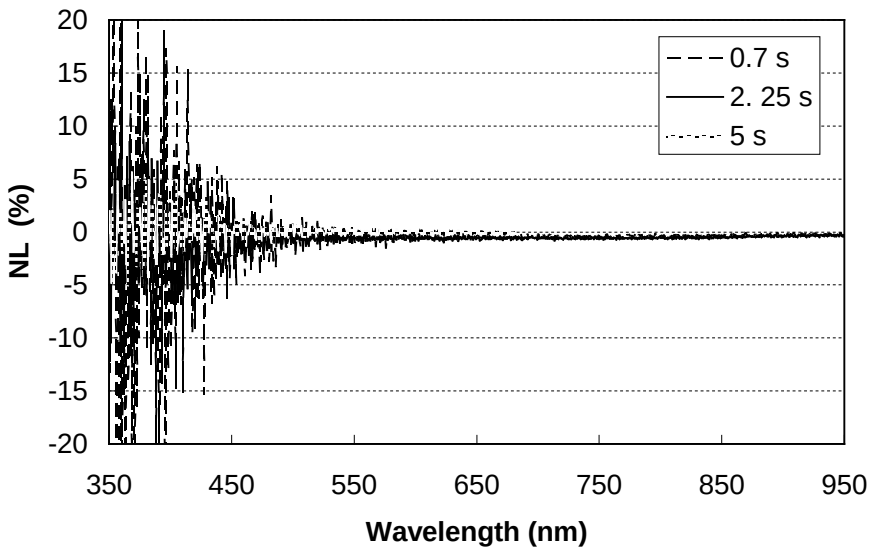

Figure 5. Nonlinearity in terms of wavelength and independently of the number of counts

4.2 Spectral stray light

Ideally, when an array detector is used in conjunction with a dispersing element, i.e., a monochromator, each pixel should detect only the radiation with the spectral content defined by the dispersing element. In practice, radiation with other spectral content, namely the “stray light”, and originating from scattered and diffracted light or from inter-reflections, can also be present. Such a contribution strongly depends on the quality of the

optical components and on the precautions put to use to reduce it. The effect of the stray light strongly depends on the application. It can be a problem when large radiation spectra are examined, because of a cumulative effect, and particularly in applications such that we are discussing because of the high dynamic of the signals. Different approaches are available to evaluate the stray light [4].

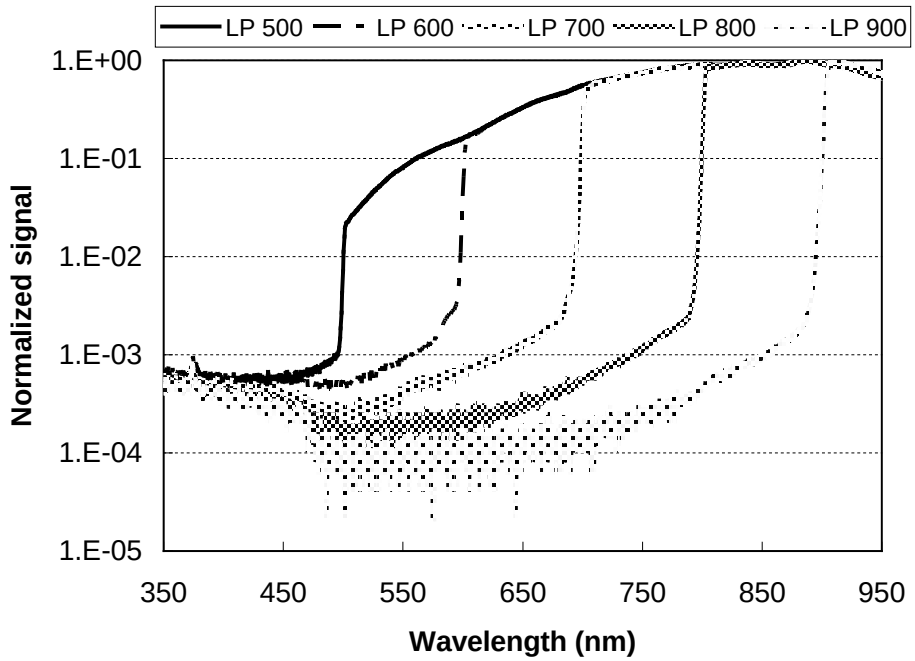

Figure 6. Normalised signals with different long-pass filters. For each filter, normalisation at maximum signal

A simplified approach making use of long pass filters of different cut-on wavelength was followed at INRIM to evaluate the stray light. A set of 5 filters with cut-on between 500 nm and 900 nm was used. All filters are such that their out-of-band transmittance at the short wavelength is not higher than $1 \cdot 10^{-6}$. Such an approach does not allow a complete characterization of the stray light contribution given to and coming from each pixel, but it is just an "application oriented" approach which can provide an estimate of the stray light.
Measurements have been performed with the blackbody source at 1400 °C and an exposure time of 1 s. The results of the characterization are presented in Figure 6.

The results are rather logical, with a progressive increase of the stray light as the cut-on move towards shorter wavelengths, i.e., as the radiance spectrum falling onto the monochromator enlarge. It can be assumed a constant contribution of about $6*10^{-4}$ with respect to the maximum over all the spectral range and consequently each measured signal will be corrected for such a figure.

4.3 Size-of-source effect

The size-of-source effect (SSE) is a typical influencing parameter of the radiation thermometers that may greatly influence the measurement accuracy. A proper design can reduce but not eliminate the effect which is a result of radiation from outside the instrument nominal target area, as defined by the field stop, reaching the detector. Usually this results in the instrument giving a higher reading as the size of the measured hot target is increased. The main causes of this effect are scattering caused by dust and other contaminants on optical surfaces, optical aberrations, scattering from imperfections within the optics and multiple reflections between components. An indirect method based on an integrating sphere apparatus was used to characterise the multi-wavelength device [5].
Figure 7 presents the results obtained at different wavelengths with progressively increased diameter of the radiating source. The resulting SSE figures have an as expected behaviour, i.e., it increases by increasing the wavelength and, even if moderately, by increasing the source diameter. The high values of SSE may depend on both imperfections of the pinhole aperture and on the use of the monochromator instead of commonly used interference filters. Such high SSE would be not compatible with applications of primary thermometry, but can be tolerated in industrial applications.

A further consideration in favour of short wavelengths operation can be derived by the curves reported in Figure 6. SSE values at 950 nm are about 50 % higher than that at 550 nm.

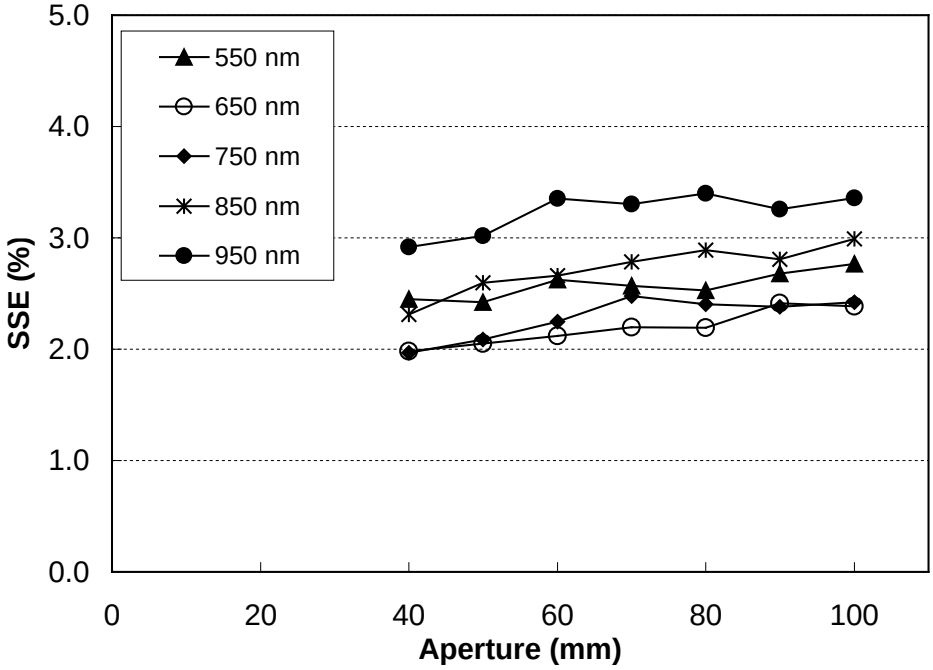

Figure 7. SSE at different wavelengths measured with a blackspot of 15 mm

In any case, it is worth to evidence that for the present exercise there is no influence of the SSE because of the approach we followed, i.e., the same radiating source has been used both to derive the spectral response curve of the MWT and to derive its temperature when a partially transmitting surface is interposed. Of course, in more general applications, a correction taking account of the dimensions of the radiating surface should be made.

4.4 Stability

Because of the measurement approach we followed, i.e., the calibration of the device in terms of spectral response curve and the use the latter to derive the spectral radiance curve of the surface under investigation, it is not important the absolute stability in terms of counts, but only that possible drifts are not spectrally dependent. The stability has been measured by using as a radiation source the same blackbody cavity already described in 4.1.1 and set to 1300 °C. Two different tests have been carried out, namely a 12 hour test and a 15 days test. Figure 8 shows a 3D representation of the relative differences on the spectral curve over 12 hours and with respect to the 1st measured curve. It can be seen that no appreciable variation occurred both with respect to the wavelength and to the time.

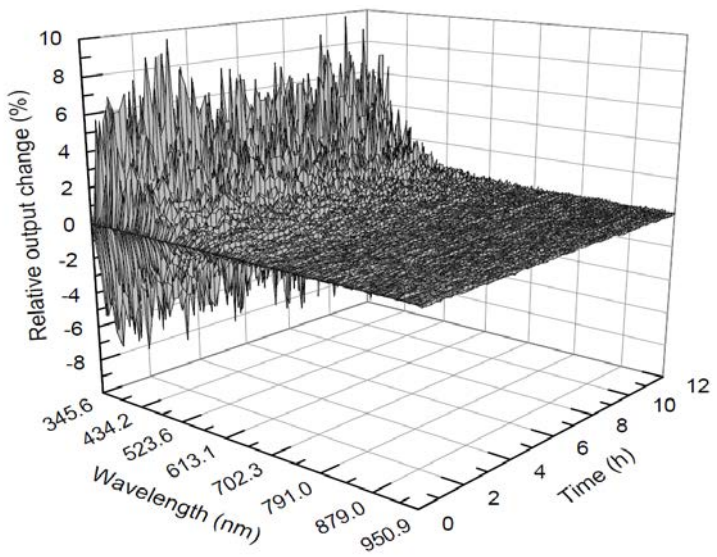

Figure 8. Variation of the output curve over a twelve hours period

The quite large dispersion at the short wavelengths is essentially due to the noise and this can be easily deduced by Figure 9 where all temporal data, namely more than 50 curves, have been averaged and the results presented in a 2D graph.

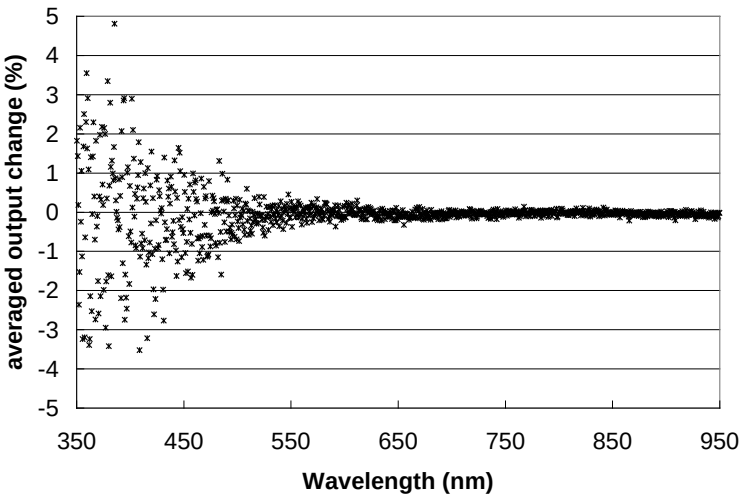

Figure 9. Averaged variation of the output curve over a twelve hours period

As for the stability test over a two weeks period, a substantial stability both with respect to the number of counts and to the wavelength was found, even if a slight dependence from the latter has been found, i.e., a variation of about 0.5 % between 500 m and 950 nm, as shown in Figure 10.

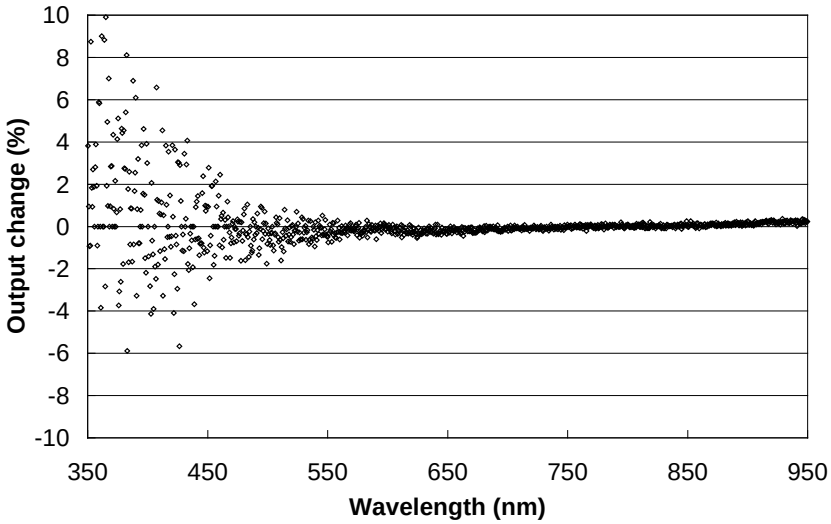

Figure 10. Variation of the output curve over a two weeks period

4.5 Spectral calibration

The spectral calibration of a row of pixels is a quite straightforward operation because all the spectral lines from a spectral lamp lying within the wavelength interval covered by the detector are acquired simultaneously. An Argon filled lamp was used and each spectral line is localised along the horizontal axis of the CCD and by reading the number of the pixel that provide the peak signal of the line. The uncertainty in the position of the peak is half the bandwidth covered by each pixel, namely 0.3 nm, when the grating with a 300 grooves/mm is used. The software of the device provide directly the indication in wavelength for each pixel. With the spectral characterisation we derive a curve of the differences between the nominal and measured wavelengths. Such differences have been fitted with a 1st order linear polynomial which residuals are always less than 0.5 nm with a standard deviation of 0.3 nm.

5. Laboratory investigations

A laboratory investigation that simulates high-temperature applications is complicated because of the difficulty in finding both suitable materials and operative heating conditions to be used. It's quite easy to heat a body within a furnace but not the same to realise a situation of freely radiating surface, i.e., without modifying the emissivity, at temperatures above 1300 °C. So it was devised a different approach. The spectral radiation emitted by a source of emissivity ε_λ at an unknown surface temperature *T* and entering the spectrometer is the same of that emitted by a blackbody at the same temperature *T* and passing through an optical window of transmittance $\tau_\lambda = \varepsilon_\lambda$ and kept at room temperature, i.e., in a not self-radiating condition. To the purpose of the measurements using a window of τ_λ in front of a blackbody is equivalent to use an heated radiating surface of emissivity ε_λ. It was so decided to use the blackbody furnace already mentioned with windows of different transmission to be interposed along the optical path furnace-thermometer. In Table 1 are summarised the different types of windows used for the trials.

Table 1. List of the windows used for the trials

No.	type of windows	details	appearance
1	optical glass BK7	thickness 4 mm	transparent
2	2 optical glasses BK7 (spaced)	thickness 4 mm each	transparent
3	4 optical glasses BK7 (spaced)	thickness 4 mm each	transparent
4	neutral filter 31.6 %	Corion AD 50 F	light grey
5	filter	no information available	medium grey
6	neutral filter M&R 3300 K	filter for carbon arc furnaces	brownish
7	neutral filter	filter for fibre optics illuminator	virtually transparent
8	polycarbonate	thickness 3 mm	transparent same as a glass

5.1 Measurement procedures

The furnace was set to 1300 °C. The radiance temperature of the blackbody cavity was measured with a precision monochromatic radiation thermometer. The thermometer was the primary standard of INRIM based on a silicon photodiode and used for the local realization of the ITS-90 with different spectral configurations. A Hamamatsu S2592-03 silicon photodiode operated in unbiased mode with a built-in Peltier cooler was used. The thermometer is a fixed focus instrument with a working distance of 675 mm with a minimum target size of 1.5 mm. For the present exercise, the spectral configuration based on a filter centred at 950 nm with a bandwidth of 70 nm was used. Once the temperature of the blackbody cavity was defined, to the purpose of comparison the radiance temperatures with and without a window interposed, were measured with both MWT and other thermometers too. A picture of the measurement setup is shown in Figure 11.

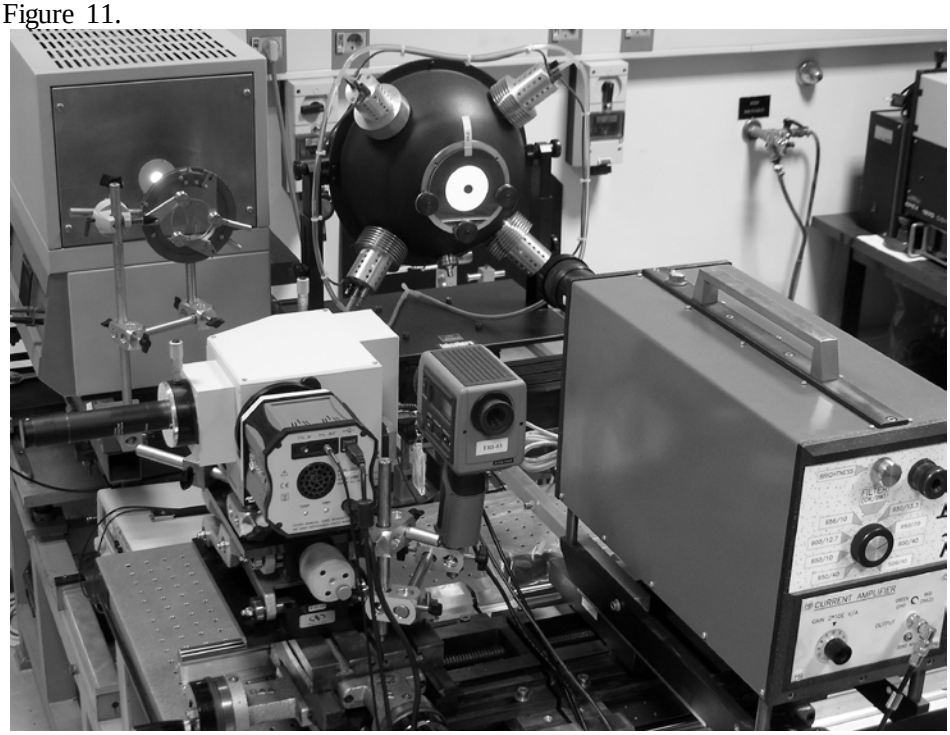

Figure 11. Picture of the measurement setup with different thermometers

The MWT was used to acquire spectra between 350 nm and 950 nm. The standard thermometer was used in two different spectral configurations with 508/10 nm and 650/10 nm interference filters, respectively, and finally a commercial good quality IR thermometer LAND model Cyclops 152 with a bandwidth comprised between 0.8 μm and 1.1 μm was used to simulate industrial applications.

The radiance temperatures at 508 nm and 650 nm have been determined from the signal ratios with respect to the furnace temperatures. It is worth to note that the measurements of the signal ratios also provide as an additional result the spectral transmittance of the different windows at 508 nm and 650 nm. Such an information is valuable because allows a direct comparison with the corresponding figures obtained, at those wavelengths, with the MWT.

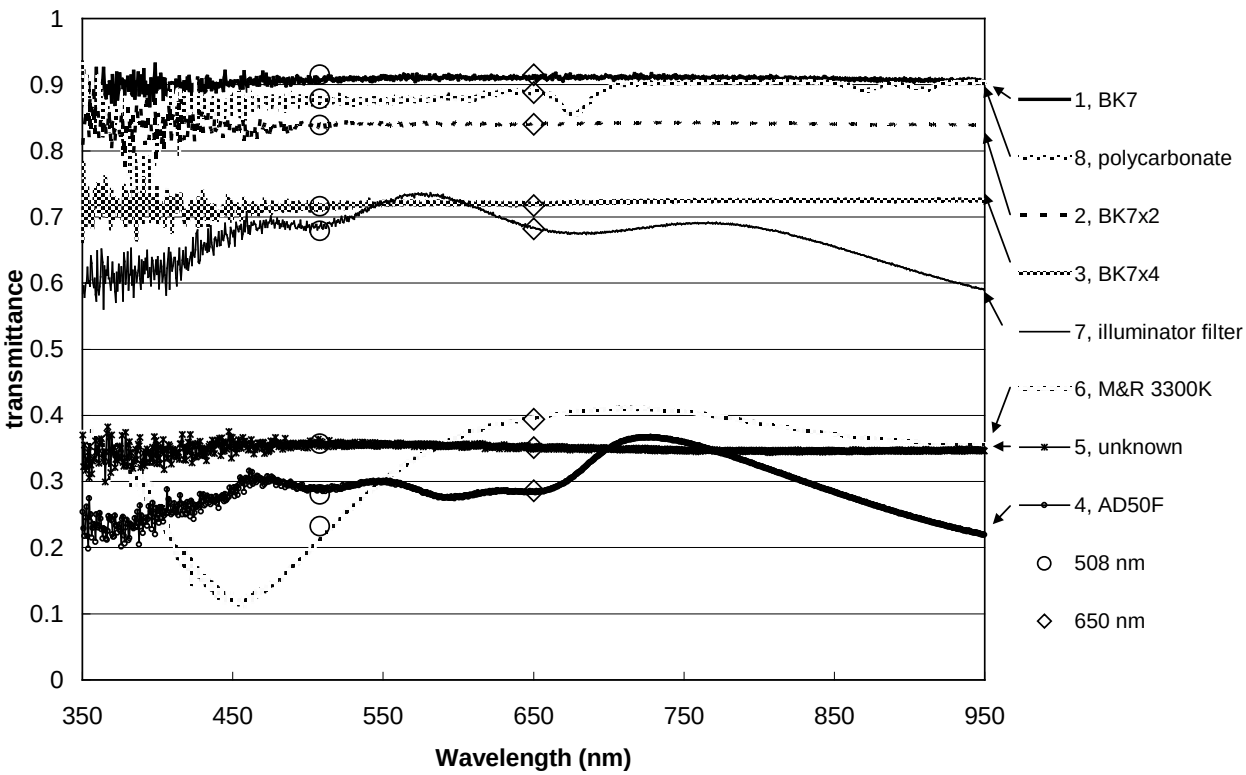

Figure 12. Transmittance spectra of the different windows as derived with the various thermometers

Figure 12 presents the different transmittance spectra obtained with the MWT overlapped the transmittance values obtained with the monochromatic thermometer at 508 nm and 650 nm. The agreement is very good, with a maximum difference of 0.024 at 508 nm with window 6 (being the others within 0.006) and always within 0.002 at 650 nm. Such results have been obtained with completely different devices, namely a standard radiation thermometer and a monochromator based multi-wavelength device, and are comfortable with respect to the results of the characterisation of the MWT.

5.2 Elaboration of the measured data

The radiance spectra acquired with the multi-wavelength device have been analysed according to the multi-wavelength approach [1]. The system of equations to be solved can be expressed and written in matrix form as:

$$\vec{Y} = \begin{bmatrix} Y_1 \\ Y_2 \\ \dots \\ Y_N \end{bmatrix} = \begin{bmatrix} c_2 & -\lambda_1 & -\lambda_1^2 & \dots & -\lambda_1^{M+1} \\ c_2 & -\lambda_2 & -\lambda_2^2 & \dots & -\lambda_2^{M+1} \\ \dots & \dots & \dots & \dots & \dots \\ c_2 & -\lambda_N & -\lambda_N^2 & \dots & -\lambda_N^{M+1} \end{bmatrix} \times \begin{bmatrix} 1/T \\ a_0 \\ \dots \\ a_M \end{bmatrix} = M \times \vec{A}$$

where $\vec{Y}$ is a N dimensional vector containing the measured data (the radiances at N different wavelengths), M is a matrix whose dimension are $(M + 2) \times N$ and containing the constant terms c_2 and the wavelengths, $\vec{A}$ is a vector of dimension $M + 2$ containing the unknowns (the temperature and the emissivity coefficients).

Finally, the vector $\vec{A}$, obtained by means of the least square method, can be expressed as follow:

$$\vec{A} = \left(M^T M\right)^{-1} M^T \vec{Y}$$

Different linear polynomials have been used, i.e., the 0th, 1st and 2nd order. A general rule was devised in the simulation exercise [1] which consists in assuming as a reliable a result when polynomials of two successive

orders give similar temperatures, namely within a specified threshold value. A threshold of 10 °C, corresponding to about ±0.3 % of *T*, was applied. It may be that the full range 350 nm - 950 nm can not be fitted with a simple linear polynomial equation, but reducing the extent of the range may facilitate to find adequate solutions to this purpose. The results considered as reliable have been averaged and are presented in Table 2.

Table 2. Errors in °C with the MWT

window	T_{furn} (°C)	$T_{multi\text{-}wavelength}$ (°C)	$T_{multi\text{-}wavelength}$ - T (°C)
1	1293.1	1291.3	-1.8
2	1296.5	1296.3	-0.2
3	1296.5	1292.2	-4.3
4	1293.2	1304.4	11.2
5	1296.5	1300.0	3.5
6	1296.5	No results	No results
7	1296.5	1285.6	-10.9
8	1297.3	1290.6	-6.7

To better clarify the procedure we adopted, we analyse the results obtained with two different windows, namely the no. 7 and no. 3. As for window no. 7, the only spectral ranges giving results within the threshold values were the 350-550 nm and the 350-600 nm with *T*=1288.0 °C and *T*=1283.2 °C, respectively. As for window no. 3, the useful spectral ranges extends also to VIS-NIR. The following ranges, i.e., 350-950 nm, 400-950 nm, 450-950 nm, 500-950 nm, 550-950 nm, 600-950 nm, 650-950 nm, 350-650 nm, gave eight temperature values which average is 1292.2 °C with a standard deviation of 3.1 °C.
It's worthwhile to stress that with all windows, but window no. 3, the VIS-NIR range 650-950 nm did not provide reliable results, i.e., results satisfying the threshold value of 10 °C for two successive order polynomials to agree. This is an extremely important point that confirms that to operate in the UV is a necessary condition to obtain reliable results. On the other hand, this is the experimental verification of the mathematical simulation performed in ref. [1] that evidenced a substantial improvement with respect to the sensitivity to the noise and to the model assumption when the spectral region was extended down to the UV. It can be recalled that it was found in [1] that enlarging the operating spectral range to 350-950 nm the errors due to random noise can be reduced by a factor more than 20 with a 2nd order polynomial.

No results are available for the window no. 6, i.e., the filter used with the carbon arc furnaces. Whichever sub-ranges has been considered, no results within the threshold has been found. This is another important point that it is worthwhile to stress. The flexibility of the approach, i.e., the great number of spectral measurement data and the possibility of analysing different spectral sub-ranges, allows to use the MWT more safely than in the past realisations. We are not sure that a reliable result can be obtained, but, when happens, the result is safe.

5.3 Comparison between multi-wavelength and single-wavelength thermometers

Table 3 summarises the radiance temperatures as measured with the single-wavelength thermometers when used with the various windows and the consequent differences with respect to the real temperature of the furnace. The radiance temperatures with the Cyclops 152 have been measured with the emissivity setting of the thermometer on ε=1 position, i.e, without any correction. The same for the measurement at 508 nm and 650 nm.

Table 3. Radiance temperatures measured with the single-wavelength thermometers

window	T_{furn} (°C)	T_{rad} (°C) @508 nm	T_{rad} (°C) @650 nm	T_{rad} (°C) @0.8-1.1μm	ΔT (°C) @508 nm	ΔT (°C) @650 nm	ΔT (°C) @0.8-1.1μm
1	1297.0	1289.3	1287.2	1281	-7.7	-9.8	-6.2
2	1296.5	1281.3	1277.3	1268	-15.2	-19.2	-28.5
3	1296.5	1268.0	1260.3	1243.5	-28.5	-36.2	-53

4	1293.2	1190.2	1165.7	1071.5	-103	-127.5	-201.7
5	1297	1212.1	1189.1	1137	-84.9	-107.9	-159.5
6	1296.5	1180.3	1199.3	1142	-116.2	-97.2	-154.5
7	1296.5	1263.5	1255.0	1208	-33.0	-41.0	-88.5
8	1297.3	1286.1	1284.2	1278	-11.2	-13.1	-19.7

Obviously, differences change if radiance temperatures are corrected for the transmittance. But, which values of transmittance should be used remains an open question. If we suppose that no information about the materials are available we may assume a prudential value of 0.5 for the transmittance. In case of windows 1, 2, 3, the appearance could help and it could be assumed them to be normal glasses with a typical transmittance of 0.92. The same for polycarbonate window that appears as transparent as a glass. By correcting the radiance temperatures reported in Table 3, the differences reported in Table 4 and in graphic form in Figure 13 have been obtained

Table 4. Temperature errors with the various thermometer after correction for the transmittance

window	**Correcting τ**	**ΔT (°C) @508 nm**	**ΔT (°C) @650 nm**	**ΔT (°C) @0.8-1.1μm**
1	0.92	-0.5	-0.6	-2
2	0.92	-8.0	-10.1	-17
3	0.92	-21.5	-27.3	-42
4	0.5	-48.6	-59.6	-133.5
5	0.5	-28.9	-36.4	-59.5
6	0.5	-62.6	-26.0	-53.5
7	0.5	27.0	35.3	22
8	0.92	-4.0	-3.9	-5.3

The results are particularly positive for the MWT being the calculated temperatures with the latter always closer to the true temperature than with the single-wavelength thermometers. Only in the case of an high emissivity, as for windows 1 and 8, the various thermometers tend to give the same results.
Anyway, in practice, the more realistic comparison is with the commercial IR thermometer @0.8-1.1μm, i.e., a type of thermometer normally used in industrial applications, being the short wavelength at 508 nm and 650 nm just as a sort of exercise, even if some short wavelength commercially available thermometer does now exist.

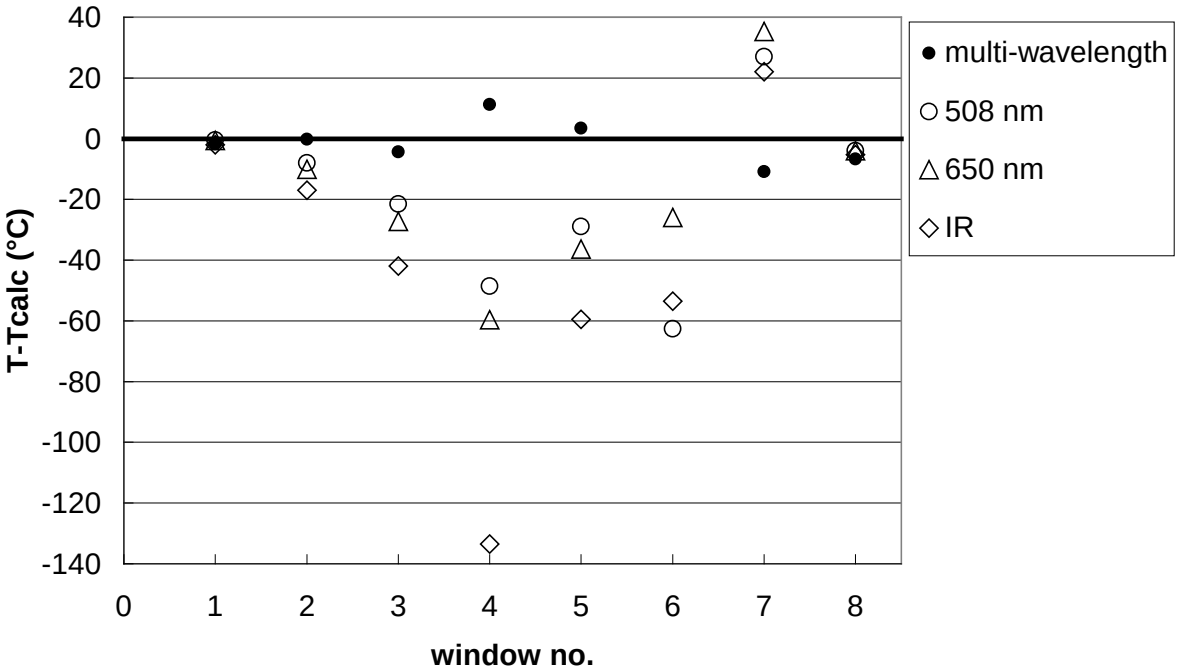

Figure 13. Temperature errors after correction for the transmittance

5.4 Measurement at 900 °C with an Inconel 600 sample

Further evidences of the advantages in the UV operation may be found in the results of a comparison exercise aimed to verify the convergence of various non-contact temperature measurement methods that was carried out within the HiTeMS project. Inconel 600 samples were selected as artefacts to be used with a maximum operating temperature of 900 °C. INRIM was able to participate to the exercise because of the unexpected high sensitivity of the multi-wavelength device which can operate down to 900 °C provided that the low wavelength limit is increased to 500 nm, i.e., a wavelength that still allows, even if partially, to take advantage of the short-wavelength operation. Because of the need to maximize the sensitivity of the apparatus the configuration was slightly different with respect to that used in the previous investigations, i.e., a 150 grooves/mm ruled grating with blaze at 500 nm and central wavelength positioned at 500 nm were adopted. Such a combined choice of the grating and of the positioning at the blaze wavelength allows the best conditions to be met at the shortest wavelengths, i.e., where signals are lower.

The experiments were conducted in a similar way to that here described, the only significant difference being the different position of the samples. In the present exercise, the samples, namely the various windows, were interposed between the furnace and the MWT, whereas during the comparison exercise the Inconel sample was mounted on a heating device and placed alongside of the furnace. The MWT was used in the spectral range from 500 nm and 950 nm to measure the surface temperature of an Inconel 600 sample (supplied by VSL) at three different temperatures, namely 880 °C, 900 C and 920 °C. To the purpose of the comparison, the true surface temperature of the sample was measured with the standard radiation thermometer at 950 nm. The spectral emissivity of the Inconel 600 sample, measured at INRIM with an high-temperature integrating sphere reflectometer, was used to correct the radiance temperature of the radiation thermometer.

The MWT was found to measure temperatures in excess of 5.1 °C, 1.2 °C, 1.4 °C at 880 °C, 900 °C, 920 °C, respectively, with respect to the standard radiation thermometer. All these results are within the estimated combined standard uncertainty of the comparison which estimate was 5.5 °C.

6. Uncertainty budget

The uncertainty to be associated to the temperatures calculated with the multi-wavelength approach can be estimated by taking into account the following components.

Temperature of the reference source:

A standard uncertainty of 0.15 °C in the measurement of the temperature of the reference blackbody cavity with the calibrated standard radiation thermometer has been assumed [6]. Such an estimate takes also into account the uncertainty in the effective emissivity of the cavity

As discussed in 4.2 a value of $6*10^{-4}$ was estimated as stray light contribution and used to correct the measured signals. Because of the rough estimation of the stray light, it can be assumed a quite high residual uncertainty of the order of $3*10^{-4}$. The way to transform the latter in a temperature uncertainty is to apply such a figure as a bias to the signals and to repeat the multi-wavelength calculations. The results are not univocal and, in any case, rather limited in extent. A maximum effect of 1.5 °C has been found with window no. 2. Precautionary, such a figure has been assumed as uncertainty contribution.

As discussed in 4.1 no appreciable non-linearity related to the number of counts is present.

Spectral calibration
A prudential uncertainty of 0.5 nm was assumed for the wavelength. Checks on the effect of assigning wrong wavelength values to the pixels were made by introducing a bias to the wavelength into the set of acquired data. The biased-data were analysed and biased-temperatures were derived. There is not a definite trend related to a shift of the wavelength values and in any case it has been found that, with shift of +/- 5 nm, a coefficient of 0.45 °C/nm was found, thus resulting in 0.23 °C for the calculated temperature.

SSE
As mentioned in 4.3 the uncertainty contribution due to the SSE is null in the present exercise, because of the approach we followed, i.e., the same radiating source used both for deriving the reference curve and for the measurement.

Repeatability
Checks were made by analysing successive runs. The dispersion of the calculated temperatures were of about 0.2 °C.

Stability
As discussed in 4.4, the device was stable during more than a working day and with a spectral drift of about 0.5 % between 500 nm and 950 nm over a period of two weeks. Assuming a prudential uncertainty of 0.25 % and transforming such a figure in radiance temperature at the different wavelengths, an estimate of some tenths of a degree, namely 0.3 °C, can be assumed.

Multi-wavelength approach
The standard deviation of the temperatures calculated with the spectral sub-ranges which give results within the assumed threshold, namely 10 °C, can be assumed as an estimate of the uncertainty of the multi-wavelength approach. An average standard deviation of about 5 °C has been found with seven of the eight different windows we tested. It is worth to note that this uncertainty component is related to the threshold value, even if in different way for the different materials.

In Table 5 are summarised the uncertainty components discussed above.

Table 5. Estimated uncertainty contributions

Source of uncertainty	**Unc. contribution u_i(y) (°C)**
Temperature of the reference source	0.15
Stray light	1.5
Linearity	Not sizeable
Spectral calibration	0.23
SSE	Not sizeable
Repeatability	0.2
Stability	0.3
Multi-wavelength approach	5

Combined standard uncertainty	5.2

The uncertainty contribution related to the multi-wavelength approach is by far the largest component with a really limited contribution of the other ones on the combined uncertainty. By adding in quadrature the different contributions a resulting combined standard uncertainty of 5.2 °C has been derived. Such a figure is rather compatible with the temperature differences found with the MWT and reported in Table 2 where only in two cases, i.e., with windows 4 and 7, the differences were a bit higher than twice the estimated uncertainty.

7. Conclusions and outlook

A spectrographic device to be used as a multi-wavelength thermometer for high-temperature industrial applications was developed at INRIM. The thermometer was based on a CCD silicon detector with rows of 1024 pixels and a dispersing monochromator. By using a 300 grooves/mm grating the apparatus was configured for operation between 350 nm and 950 nm at temperatures from 1300 °C up and from 900 °C up when the low working wavelength is increased to 500 nm. The thermometer was characterized in terms of spectral response, size-of-source effect, linearity, stray light and an uncertainty budget was calculated and a standard uncertainty of 5.2°C at 1300 °C was estimated.

The MWT was used in a laboratory investigation to test its suitability to derive correctly the temperature of a blackbody cavity at 1300 °C when it was observed through optical windows with unknown transmittance. It was found that when a reliable result can be obtained, i.e., the calculated temperatures with different fitting polynomials are within a selected threshold value, differences with respect to the real source temperature are always well within 1 % of *T*. It is worth to evidence that, differently from past realizations of MWT in the visible or near-infrared, to operate down to 350 nm with flexible spectral ranges provides additional information which allow to decide on the acceptance or not of a result. A general rule was devised in the simulation exercise [1] which consists in assuming as a reliable a result when linear polynomials of two successive orders give similar temperatures, namely within a specified threshold value. A threshold of 10 °C, corresponding to about ±0.3 % of *T*, was applied in the present exercise and it was found that generally the full range 350 nm - 950 nm can not be fitted with a simple linear polynomial equation, but reducing the extent of the range facilitates to find a reliable result. It is an important point which remove one of the major weak points of the multi-wavelength approach, i.e., the unpredictability of the possible errors. It can not be taken for granted that a result is obtained, but when this happens such a result is a reliable one.

The MWT and other three single-band thermometers, at 508 nm, 650 nm and (800 -1100) nm, were also used in a performance comparison. The radiance temperatures measured with the single-band thermometers have been corrected for “estimated transmittance”, i.e., by assigning reasonable values to the unknown transmittance of the windows. In all cases that the MWT is able to give a reliable result, the latter was more precise than with the single-band thermometers for which errors as large as some tens of degrees Celsius, and up to more than 130 °C, may be encountered.

A different version of the MWT based on a linear silicon photodiode array (PDA) and with a refractive input optics is already planned. A suitable PDA, which was not available when the device was designed, should facilitate the characterization and allow to manage with a flexible grouping the spectral arrangement of the pixels and particularly at the short wavelengths where the signals are low.

Acknowledgements

The EMRP is jointly funded by the EMRP participating countries within EURAMET and the European Union.

The research within this EURAMET joint research project receives funding from the European Community’s Seventh Framework Programme, ERA-NET Plus, under Grant Agreement No. 217257.

References

[1] Battuello M, Girard F 2014 *Int J Thermophys* DOI: 10.1007/s10765-014-1678-1

[2] Coates P B 1981 *Metrologia* **17** 103-109

[3] Battuello M, Bloembergen P, Girard F, Ricolfi T 2003 *Temperature: Its Measurement and Control in Science and Industry AIP* **7** 613-8
[4] Salim S G R, Fox N P, Hartee W S, Woolliams E R, Sun T and Grattan T V 2011 *Applied Optics* **50** 5130-8
[5] Lowe D, Battuello M, Machin G and Girard F 2003 *Temperature: Its Measurement and Control in Science and Industry AIP* **7** 613-8
[6] Battuello M, Girard F and Florio M 2009 *Metrologia* **46** 26-32

Highlights

A novel flexible UV multi-wavelength thermometer was developed and characterized
The UV operation drastically reduce the possible errors of the multi-wavelength approach
A general rule has been developed that confirms the reliability of the results

A result is not guaranteed but when obtained it is with a good level of confidence.